



Published in final edited form as:

Eur J Med Chem. 2019 July 01; 173: 32–43. doi:10.1016/j.ejmech.2019.03.065.

Development of CXCR4 modulators based on the lead compound RB-108

Renren Bai^{a,*}, Xiaokang Jie^a, Jian Sun^a, Zhongxing Liang^b, Younghyoun Yoon^b, Amber Feng^b, Yoonhyeun Oum^b, Wenyan Yu^a, Rui Wu^a, Bin Sun^c, Eric Salgado^b, Yuanyuan Xie^{a,c}, and Hyunsuk Shim^{b,d,*}

^aCollege of Pharmaceutical Science, Zhejiang University of Technology, Hangzhou, China

^bDepartment of Radiation Oncology, Emory University School of Medicine, Atlanta, Georgia, USA

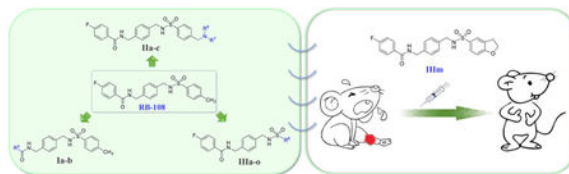
^cKey Laboratory for Green Pharmaceutical Technologies and Related Equipment of Ministry of Education, Zhejiang University of Technology, Hangzhou, China

^dWinship Cancer Institute, Emory University, Atlanta, Georgia, USA

Abstract

The CXCR4/CXCL12 axis plays prominent roles in tumor metastasis and inflammation. CXCR4 has been shown to be involved in a variety of inflammation-related diseases. Therefore, CXCR4 is a promising potential target to develop novel anti-inflammatory agents. Taking our previously discovered CXCR4 modulator RB-108 as the lead compound, a series of derivatives were synthesized structurally modifying and optimizing the amide and sulfamide side chains. The derivatives successfully maintained potent CXCR4 binding affinity. Furthermore, compounds **IIIb**, **IIIc**, **IIIg**, **IIIj**, and **IIIm** were all efficacious in inhibiting the invasion of CXCR4-positive cells, displaying a much more potent effect than the lead compound RB-108. Notably, compound **IIIm** significantly decreased carrageenan-induced swollen volume and paw thickness in a mouse paw edema model. More importantly, **IIIm** exhibited satisfying PK profiles with a half-life of 4.77 h in an SD rat model. In summary, we have developed compound **IIIm** as a new candidate for further investigation based on the lead compound RB-108.

Graphic abstract



*Corresponding authors **Hyunsuk Shim**, Department of Radiation Oncology, Emory University School of Medicine, 1701 Uppergate Drive, C5018, Atlanta, GA, USA, 30322. hshim@emory.edu, **Renren Bai**, College of Pharmaceutical Science, Zhejiang University of Technology, 18 Chaowang Road, Hangzhou, Zhejiang, China, 310014. renrenbai@zjut.edu.cn.

Publisher's Disclaimer: This is a PDF file of an unedited manuscript that has been accepted for publication. As a service to our customers we are providing this early version of the manuscript. The manuscript will undergo copyediting, typesetting, and review of the resulting proof before it is published in its final citable form. Please note that during the production process errors may be discovered which could affect the content, and all legal disclaimers that apply to the journal pertain.

Keywords

CXCR4 modulators; RB-108; structural modification; Inflammatory cell recruitment; Anti-inflammation

1. Introduction

The chemokine receptor CXCR4 is a seven transmembrane G protein-coupled receptor [1]. CXCR4 is widely expressed throughout the human body during the embryonic development and through adult life. Its cognate ligand is the chemokine CXCL12 (also named stromal cell-derived factor-1 α , SDF-1 α) [2, 3]. Given its prominent roles in tumor metastasis and inflammation, CXCR4 has gained plenty of attention in the recent decade [4-7]. Evidence has proven that the CXCR4/CXCL12 axis can chemotactically recruit inflammatory cells (neutrophils, monocytes, and lymphocytes) to local tissues and regulate the release of inflammatory factors that cause inflammatory responses [8, 9]. CXCR4 has been found to be involved in a variety of inflammation-related diseases. For example, in rheumatoid arthritis, CXCR4-expressing CD4⁺ memory T cells accumulate in the inflamed synovium due to the locally increased CXCL12 concentration [10]. Moreover, it has also been shown that CXCR4/CXCL12 axis plays an important role in skin inflammation, the cutaneous expression of both CXCL12 and CXCR4 was upregulated in the inflamed skin of K14-VEGF-A transgenic mice and in imiquimod-induced skin inflammation [11]. Therefore, CXCR4 is a promising potential target for the treatment of inflammatory diseases.

AMD3100 with a bicyclam moiety was the first small molecule CXCR4 antagonist entering clinical trials for the treatment of HIV infection, but it was not approved due to serious cardiotoxicity [12-16]. Taking AMD3100 as the lead compound, our research group discovered a series of promising bis-secondary amines as potent CXCR4 antagonist, including Q-122, a CXCR4 modulator which is now under Phase IIb clinical trials on neuroinflammation indication [17]. Further structural modification and optimization of the two secondary amine groups lead to the discovery of the second generation of CXCR4 modulators, the amide-sulfamide compounds [18, 19]. Among these amide-sulfamide derivatives, RB-108 displayed potent *in vitro* and *in vivo* anti-inflammatory activity and was selected as our lead compound. To further improve its anti-inflammatory activity, we performed structural modification and optimization of the amide and sulfamide side chains of RB-108. The CXCR4 binding affinity, anti-CXCR4 activities, *in vivo* anti-inflammatory activity, pharmacokinetic properties, and the cytotoxicity of the RB-108 derivatives were systematically evaluated.

2. Results and discussion

2.1. Chemistry

The synthetic route to synthesize compounds **Ia-b** is outlined in Scheme 1. Intermediate **2** was synthesized by sulfonylation of the starting material 4-(Boc-aminomethyl)benzylamine (**1**) with 4-methylbenzenesulfonyl chloride in dichloromethane (DCM). The protective group Boc was subsequently removed in the presence of trifluoroacetic acid (TFA) producing the

benzylamine intermediate **3**. The final compounds **Ia-b** were prepared by the acylation of intermediate **3** with corresponding benzoic acid derivatives.

The synthetic route to prepare compounds **IIa-c** was shown in Scheme 2. Intermediate **4** was synthesized by sulfonylation of **1** with 4-(bromomethyl)benzenesulfonyl chloride in DCM. The benzyl bromide group reacted with secondary amine derivatives producing compounds **5a-c**. The protective group Boc was subsequently removed in the presence of TFA to provide intermediates **6a-c**. The final compounds **IIa-c** were prepared by the acylation of intermediate **6a-c** with 4-fluorobenzoic acid.

The synthetic route to prepare compounds **IIIa-o** was summarized in Scheme 3. All the targeted compounds were prepared according to the similar reaction conditions in Scheme 1 and Scheme 2.

2.2. Preliminary binding affinity screening

All of the prepared compounds were first screened with a binding affinity assay as described in our previous publications [18-23]. The screening protocol is a competitive CXCR4 binding assay between biotinylated TN14003, a potent CXCR4 peptidic antagonist, and the target compounds **Ia-b**, **IIa-c**, and **IIIa-o** at concentrations of 1, 10, 100, and 1000 nM. The effective concentration (EC) is used to measure the affinity, which is defined as the lowest concentration at which a reduction in the rhodamine fluorescent color, suggesting superior binding affinity of our testing compounds compared to TN14003, is observed as compared to control (Fig. 3). Thus, this initial screening is a semi-quantitative, primary screening of the level of activity, which is different from IC₅₀. Through CXCR4 binding affinity testing of hundreds of compounds, we have found that compounds with EC values of up to 100 nM can be considered as promising compounds showing potent affinities, likely to becoming potential candidate compounds and worthy for further investigation.

As shown in Table 1 and Fig. 2, by introducing a nitrogen atom into the side chain of the amide structure, this resulted in a significant decrease in the receptor affinity. Compared with RB-108, the EC of compounds **Ia** and **Ib** is reduced by more than 1000-fold, with ECs of 1000 and >1000 nM, respectively, equivalent to the reference compound AMD3100 (EC = 1000 nM). Secondly, the sulfamide group was well tolerated, and different electron withdrawing and electron donating substituents showed no absolute impact on the affinity, as the ECs of most derivatives were much more potent than that of AMD3100. When the sulfonamide benzene ring was substituted with an aliphatic secondary amine, the EC of the compounds **IIa-c** was only 1 nM, which was as potent as RB108 and 1000-fold more effective than that of AMD3100. However, the activity was significantly decreased after the introduction of the nitrogen atom in the sulfonamide benzene ring (EC of **III** was 1000 nM), while compound **III**m (EC = 10 nM) possessing an oxygen-containing heterocyclic ring showed good affinity. Additionally, when the sulfonamide side chain was substituted, the melting points of most of the compounds were significantly lower than that of RB-108, showing much better water solubility.

2.3. Matrigel invasion assay

Activation of chemokine receptor CXCR4 through its chemokine ligand CXCL12 mediates migration and invasion of CXCR4-positive cells. Therefore, a Matrigel invasion model was utilized to as the primary functional assay to probe whether the selected compounds through binding affinity assay (no more than 100 nM) can block CXCR4/CXCR12 mediated chemotaxis and invasion [20, 23]. The selected compounds and CXCR4-positive MDA-MB-231 human breast cancer cells were added to the upper chamber of a vessel and CXCL12 was added to the lower chamber as a chemoattractant in serum-free medium. Binding of CXCR4 at the cell surface with the selected compounds would interfere with CXCL12-mediated chemotaxis. Inhibition of cell invasion with each tested compound was calculated by comparing results to the cell invasion without treatment.

As expected, compounds with better CXCR4 affinity exhibited excellent efficacy in reducing CXCR4-positive cell invasion (Fig. 3). Except for compounds **IIIc**, **IIIe** and **IIIo**, the anti-CXCR4 activity of other compounds was significantly much more potent than that of AMD3100 (55%), and even exceeded that of the other positive control RB-108 (65%). Among them, the inhibitory activity of compounds **Iib**, **Iic**, **IIIg**, **IIIj** and **IIIm** (92%, 82%, 95%, 93% and 83%, respectively) indisputably exceeded the anti-CXCR4 activity of the lead compound RB-108. Fig. 4 obviously proved that these anti-CXCR4 compounds effectively blocked the invasive function of CXCR4 pathway, as the number of invading cells to the bottom chamber significantly decreased compared to the negative control, and much less than that of AMD3100 and RB-108.

Collectively, the structural modification based on RB-108 was successfully performed in this work. By modifying the amide and sulfamide groups, especially the sulfamide side chain, candidate compounds with more significant antagonism to the CXCR4/CXCL12 pathway were obtained.

2.4. *In vivo* anti-inflammatory activity against carrageenan-induced paw edema

Previously, we reported utilizing a carrageenan-induced mouse paw edema model as an efficient model to evaluate the *in vivo* anti-CXCR4 activity [17, 20]. This model is widely used to assess anti-inflammatory activity *in vivo*. On the basis of the *in vitro* assay results, 5 compounds (**Iib**, **Iic**, **IIIg**, **IIIj** and **IIIm**) with the most potent anti-CXCR4-positive cell invasive activity were selected to investigate their suppressive effect on acute inflammation. Because of the *in vivo* toxicity of AMD3100, we selected the lead compound RB-108 as the reference drug for our animal experiments [17, 24].

In previous experiments, some compounds highly active *in vitro* did not exhibit positive anti-inflammatory activity *in vivo*. However, as illustrated in Fig. 5, all of the selected compounds derived from RB-108 showed favorable anti-inflammatory activity. Compounds **Iib**, **Iic**, **IIIg** and **IIIj** inhibited the swelling of the mouse paw by approximately 20%. Their potencies were weaker than that of the positive control RB-108 (30%). However, the sulfamide side chain modified compound **IIIm** exhibited the most potent activity against mouse paw edema with 43% inhibition, which was more potent than the lead compound

RB-108. The swollen volume and paw thickness were obviously reduced in the **III**m treated group (Fig. 6).

To further microscopically analyze the anti-inflammatory activity of compound **III**m and investigate its effects on inflammatory tissues, histological analysis of the mouse paw was performed. As shown in Fig. 7, the dermis of normal mouse paw tissue is tightly connected to the epidermis through a basement membrane, and the papillary region is composed of loose areolar connective tissue (**A1-2**). However, the carrageenan-induced inflammatory tissue showed intense dermal papillae edema, with a huge number of inflammatory cells penetrating into the inflammatory tissue through dilated blood vessels (**B1-2**). Compound **III**m notably attenuated the inflammation and tissue damage in the mouse paw, as both the edema volume and thickness of mouse paw were notably reduced (**C1-2**). More importantly, the number of inflammatory cells accumulated in the tissue was markedly decreased after treatment with **III**m. These positive results further confirm that our compounds can effectively block inflammatory cell accumulate in the inflammatory tissues, which is the main anti-inflammatory pathway involving CXCR4.

2.5. Preliminary pharmacokinetic profiles study of compound **III**m

Besides potency, the pharmacokinetic (PK) properties are also key factors in determining the *in vivo* feasibility of a compound. Based on the comprehensive *in vivo* anti-inflammatory activity, the preliminary PK properties of compound **III**m were tested in an SD rat model. Compound **III**m was administered via intragastric administration at doses of 10 mg/kg. After administration, blood samples were collected at 7 time points including 5 min, 15 min, 30 min, 1 h, 2 h, 4 h and 6 h for analyses with LC/MS/MS [25]. Notably, **III**m exhibited satisfying PK profiles with a half-life ($T_{1/2}$) of 4.77 h and a time to peak (T_{max}) of 0.25 h (Fig. 8). Therefore, **III**m becomes a favorable candidate for further study.

2.6. Preliminary cytotoxicity evaluation of compound **III**m

To preliminarily evaluate the safety of compound **III**m, its cytotoxicity was evaluated on three representative human breast cancer cell lines, MDA-MB-231, SKBR3 and MCF-10A, by a cell viability (MTT) assay. Compound **III**m displayed potent CXCR4 binding affinity at only 10 nM, however, it did not inhibit the proliferation of MDA-MB-231, SKBR3 and MCF-10A cells even at concentrations as high as 100 μ M (Fig. 9), a 10000-fold higher than the working concentrations. Generally, **III**m did not display observable cytotoxicity.

3. Conclusion

CXCR4 is a potential target for the development of novel anti-inflammatory agents with different mechanism from traditional nonsteroidal anti-inflammatory drugs. To further improve the anti-inflammatory activity of the lead compound RB-108, we performed structural modification and optimization of the amide and sulfamide side chains, and systematically evaluated the *in vitro* and *in vivo* anti-inflammatory activity of the derivatives. Among them, compound **III**m exhibited a much more potent effect than RB-108 in the treatment of inflammation both *in vitro* and *in vivo*. **III**m notably blocked the acute inflammation of mouse paw by 43% and attenuated tissue damage. More importantly, the

number of inflammatory cells in the paw tissue was markedly decreased after being treated with **IIIIm**. These positive results also further confirm the main anti-inflammatory mechanism of our CXCR4 modulators. In addition to its promising potency, **IIIIm** also showed satisfying PK properties with a half-life ($T_{1/2}$) of 4.77 h in rats.

4. Experimental section

4.1. Chemistry

4.1.1. General information—Proton and carbon NMR spectra were recorded on INOVA-400 (400 MHz) or VNMR-400 spectrometers. The spectra obtained in DMSO- d_6 were referenced to the residual solvent peak. Chemical shifts (δ) are reported in parts per million (ppm) relative to residual undeuterated solvent as an internal reference. Mass spectra were recorded on a JEOL spectrometer at Emory University Mass Spectrometry Center. Analytical thin layer chromatography (TLC) was performed on precoated glass backed plates from Scientific Adsorbents Incorporated (Silica Gel 60 F254; 0.25 mm thickness).

4.1.2. Procedure for synthesis of intermediate 2—A solution of 4-(Boc-aminomethyl)benzylamine (**1**) (1.0 mmol) and TEA (3.0 mmol) in anhydrous DCM (8 mL) was cooled with an ice bath, then 4-methylbenzenesulfonyl chloride (1.1 mmol, dissolved in 2 mL anhydrous DCM) was added dropwise. The reaction mixture was allowed to stir at 0 °C for 2 h. After removing the cooling bath, the resulting mixture was stirred for 5 h at room temperature, then diluted with saturated aqueous NaHCO₃ and extracted with DCM (10 mL) three times. The combined organic layer was sequentially washed with water and brine, dried with anhydrous Na₂SO₄, and concentrated in vacuo. The crude was purified by column chromatography with DCM/methanol (150:1, v/v) to yield the product as a white solid.

4.1.3. Procedure for synthesis of intermediate 3—A solution of intermediates **2** (1.0 mmol) in DCM (10 mL) was treated with TFA (4.0 mmol) at room temperature. The resulting mixture was stirred for 8 h. The solvent was removed under reduced pressure. The residue was dissolved in saturated aqueous NaHCO₃ (2 mL) followed by adding more saturated aqueous NaHCO₃ to adjust to pH = 10. Then, the mixture was filtered and the intermediate **3** was obtained as a white filter cake without further purification.

4.1.4. General procedure for synthesis of target compounds la-b—To a solution of intermediate **3** (1.0 mmol), hydroxybenzotriazole (HOBT, 1.2 mmol), 1-ethyl-3-(3-dimethylaminopropyl)carbodiimide (EDCI, 1.2 mmol) and TEA (3.0 mmol) in anhydrous DCM (8 mL), corresponding benzoic acid derivatives (1 mmol) was added. The reaction mixture was stirred for 16 h at room temperature, then diluted with saturated aqueous NaHCO₃ and extracted with DCM (10 mL) three times. The combined DCM layer was sequentially washed with water and brine, dried with anhydrous Na₂SO₄, and concentrated in vacuo. The crude was purified by column chromatography with DCM/methanol (50:1, v/v) to give the compounds as white solids.

4.1.4.1. 5-Fluoro-N-(4-(((4-methylphenyl)sulfonamido)methyl)benzyl)picolinamide

(Ia): White solid, yield 75%, m.p. 133-135 °C. ¹H NMR (400 MHz, DMSO-*d*₆) δ 9.29 (t, *J* = 6.4 Hz, 1H), 8.65 (d, *J* = 2.8 Hz, 1H), 8.11 (dd, *J* = 8.8, 4.7 Hz, 1H), 8.02 (t, *J* = 6.4 Hz, 1H), 7.88 – 7.93 (m, 1H), 7.67 (d, *J* = 8.2 Hz, 2H), 7.36 (d, *J* = 8.2 Hz, 2H), 7.23 (d, *J* = 8.2 Hz, 2H), 7.16 (d, *J* = 8.1 Hz, 2H), 4.43 (d, *J* = 6.4 Hz, 2H), 3.89 (d, *J* = 6.3 Hz, 2H), 2.36 (s, 3H). ¹³C NMR (100 MHz, DMSO-*d*₆) δ 162.88, 161.92, 159.36, 146.70, 142.50, 138.37, 137.74, 136.92, 136.67, 136.10, 129.53, 127.51, 127.23, 126.48, 124.51, 124.33, 124.15, 124.09, 45.88, 42.15, 20.90. HRMS calcd for C₂₁H₂₁O₃N₃SF 414.12822 [M + H]⁺, found 414.12812.

4.1.4.2. 6-Fluoro-N-(4-(((4-methylphenyl)sulfonamido)methyl)benzyl)nicotinamide

(Ib): White solid, yield 60%, m.p. 186-188 °C. ¹H NMR (400 MHz, DMSO-*d*₆) δ 9.24 (t, *J* = 5.9 Hz, 1H), 8.73 (d, *J* = 1.9 Hz, 1H), 8.42 (td, *J* = 8.2, 2.5 Hz, 1H), 8.04 (t, *J* = 6.3 Hz, 1H), 7.68 (d, *J* = 8.2 Hz, 2H), 7.38 (d, *J* = 7.9 Hz, 2H), 7.31 (dd, *J* = 8.6, 2.7 Hz, 1H), 7.25 (d, *J* = 7.9 Hz, 2H), 7.19 (d, *J* = 7.8 Hz, 2H), 4.45 (d, *J* = 5.9 Hz, 2H), 3.91 (d, *J* = 6.2 Hz, 2H), 2.37 (s, 3H). ¹³C NMR (100 MHz, DMSO-*d*₆) δ 165.37, 163.53, 162.98, 147.42, 147.26, 142.52, 141.43, 141.34, 138.05, 137.76, 136.31, 129.55, 128.54, 127.56, 127.20, 126.49, 109.59, 109.21, 45.84, 42.38, 20.91. HRMS calcd for C₂₁H₂₁O₃N₃SF 414.12822 [M + H]⁺, found 414.12820.

4.1.5. Procedure for synthesis of intermediate 4—A solution of 4-(Boc-aminomethyl)benzylamine (**1**) (1.0 mmol) and TEA (3.0 mmol) in anhydrous DCM (8 mL) was cooled with an ice bath, then 4-(bromomethyl)benzenesulfonyl chloride (1.1 mmol, dissolved in 2 mL anhydrous DCM) was added dropwise. The reaction mixture was allowed to stir at 0 °C for 2 h. After removing the cooling bath, the resulting mixture was stirred for 6 h at room temperature, then diluted with saturated aqueous NaHCO₃ and extracted with DCM (10 mL) three times. The combined organic layer was sequentially washed with water and brine, dried with anhydrous Na₂SO₄, and concentrated in vacuo. The crude **4** was purified by column chromatography with DCM/methanol (200:1, v/v) to yield the product as a white solid.

4.1.6. General procedure for synthesis of intermediate 5a-c—To a solution of intermediate **4** (1.0 mmol) and K₂CO₃ (2.0 mmol) in acetonitrile (10 mL), corresponding secondary amine derivative (4.0 mmol) was added, and the mixture was stirred at reflux for 4 h. The resulting mixture was filtered, and the filtrate was concentrated in vacuo. The crude was purified by column chromatography with DCM/methanol (100:1, v/v) to give the product **5a-c** as white solids.

4.1.7. General procedure for synthesis of intermediates 6a-c—A solution of **5a-c** (**2**) (1.0 mmol) in DCM (10 mL) was treated with TFA (4.0 mmol) at room temperature. The resulting mixture was stirred for 8 h. The solvent was removed under reduced pressure. The residue was dissolved in saturated aqueous NaHCO₃ (2 mL) followed by adding more saturated aqueous NaHCO₃ to adjust to pH = 10. Then, the mixture was filtered and the intermediates **6a-c** was obtained as the white filter cake without further purification.

4.1.8. General procedure for synthesis of target compounds IIa-c—To a solution of intermediates **6a-c** (1.0 mmol), HOBT (1.2 mmol), EDCI (1.2 mmol) and TEA (3.0 mmol) in anhydrous DCM (8 mL), 4-fluorobenzoic acid (1.0 mmol) was added. The reaction mixture was stirred for 16 h at room temperature, then diluted with saturated aqueous NaHCO₃ and extracted with DCM (10 mL) three times. The combined DCM layer was sequentially washed with water and brine, dried with anhydrous Na₂SO₄, and concentrated in vacuo. The crude was purified by column chromatography with DCM/methanol to give the compounds **IIa-c** as white solids.

4.1.8.1. N-(4-(((4-((diethylamino)methyl)phenyl)sulfonamido)methyl)benzyl)-4-fluorobenzamide (IIa): White solid, yield 84%, m.p. 143-145 °C. ¹H NMR (600 MHz, DMSO-*d*₆) δ 9.03 (t, *J* = 6.0 Hz, 1H), 8.06 (t, *J* = 6.3 Hz, 1H), 7.92 – 7.98 (m, 2H), 7.73 (d, *J* = 8.3 Hz, 2H), 7.49 (d, *J* = 8.2 Hz, 2H), 7.30 (t, *J* = 8.9 Hz, 2H), 7.21 (d, *J* = 8.2 Hz, 2H), 7.15 (d, *J* = 8.1 Hz, 2H), 4.42 (d, *J* = 6.0 Hz, 2H), 3.95 (d, *J* = 6.2 Hz, 2H), 2.45 (q, *J* = 7.1 Hz, 4H), 0.97 (t, *J* = 7.1 Hz, 6H). ¹³C NMR (150 MHz, DMSO-*d*₆) δ 165.03, 164.68, 163.03, 145.13, 138.97, 138.49, 136.17, 130.78, 130.76, 129.88, 129.82, 128.84, 127.61, 127.52, 127.09, 127.03, 126.37, 115.27, 115.12, 56.38, 46.32, 45.86, 42.36, 11.66. HRMS calcd for C₂₆H₃₁O₃N₃SF 484.2065 [M + H]⁺, found 484.2084.

4.1.8.2. N-(4-(((4-(pyrrolidin-1-ylmethyl)phenyl)sulfonamido)methyl)benzyl)-4-fluorobenzamide (IIb): White solid, yield 77%, m.p. 151-153 °C. ¹H NMR (600 MHz, DMSO-*d*₆) δ 9.04 (t, *J* = 6.0 Hz, 1H), 8.07 (t, *J* = 6.3 Hz, 1H), 7.94 – 7.96 (m, 2H), 7.73 (d, *J* = 8.3 Hz, 2H), 7.48 (d, *J* = 8.0 Hz, 2H), 7.30 (t, *J* = 8.8 Hz, 2H), 7.21 (d, *J* = 8.0 Hz, 2H), 7.15 (d, *J* = 8.1 Hz, 2H), 4.42 (d, *J* = 5.9 Hz, 2H), 3.94 (d, *J* = 6.0 Hz, 2H), 3.62 (s, 2H), 2.42 (s, 2H), 1.68 – 1.71 (m, 4H). ¹³C NMR (150 MHz, DMSO-*d*₆) δ 165.04, 164.68, 163.03, 144.30, 130.79, 130.77, 139.07, 138.49, 136.14, 129.82, 128.88, 127.54, 127.10, 126.44, 115.28, 115.13, 58.94, 53.48, 45.87, 42.36, 23.14. HRMS calcd for C₂₆H₂₉O₃N₃SF 482.1908 [M + H]⁺, found 482.1930.

4.1.8.3. N-(4-(((4-(morpholinomethyl)phenyl)sulfonamido)methyl)benzyl)-4-fluorobenzamide (IIc): White solid, yield 78%, m.p. 165-167 °C. ¹H NMR (600 MHz, DMSO-*d*₆) δ 9.04 (t, *J* = 6.0 Hz, 1H), 8.08 (t, *J* = 6.3 Hz, 1H), 7.94 – 7.96 (m, 2H), 7.74 (d, *J* = 8.2 Hz, 2H), 7.49 (d, *J* = 8.1 Hz, 2H), 7.30 (t, *J* = 8.8 Hz, 2H), 7.21 (d, *J* = 8.0 Hz, 2H), 7.15 (d, *J* = 8.1 Hz, 2H), 4.42 (d, *J* = 5.9 Hz, 2H), 3.94 (d, *J* = 6.2 Hz, 2H), 3.58 (t, *J* = 4.6 Hz, 4H), 3.52 (s, 2H), 2.35 (s, 4H). ¹³C NMR (150 MHz, DMSO-*d*₆) δ 165.05, 164.68, 163.03, 142.71, 139.34, 138.50, 136.13, 130.78, 130.76, 129.88, 129.82, 129.31, 127.53, 127.41, 127.40, 127.10, 126.46, 115.28, 115.13, 66.15, 61.66, 53.12, 45.86, 42.36. HRMS calcd for C₂₆H₂₉O₄N₃SF 498.1857 [M + H]⁺, found 498.1871.

4.1.9. Procedure for synthesis of intermediate 7—To a solution of 4-(Boc-aminomethyl)benzylamine (**1**) (1.0 mmol), HOBT (1.2 mmol), EDCI (1.2 mmol) and TEA (3.0 mmol) in anhydrous DCM (8 mL), 4-fluorobenzoic acid (1.0 mmol) was added. The reaction mixture was stirred for 16 h at room temperature, then diluted with saturated aqueous NaHCO₃ and extracted with DCM (10 mL) three times. The combined DCM layer was sequentially washed with water and brine, dried with anhydrous Na₂SO₄, and

concentrated in vacuo. The crude was purified by column chromatography with DCM/methanol to give intermediate **7** as a white solid.

4.1.10. Procedure for synthesis of intermediate 8—A solution of intermediate **7** (1.0 mmol) in DCM (10 mL) was treated with TFA (4.0 mmol) at room temperature. The resulting mixture was stirred for 8 h. The solvent was removed under reduced pressure. The residue was dissolved in saturated aqueous NaHCO₃ (2 mL) followed by adding more saturated aqueous NaHCO₃ to adjust to pH = 10. Then, the mixture was filtered and the intermediate **8** was obtained as the white filter cake without further purification.

4.1.11. General procedure for synthesis of compounds IIIa-o—A solution of intermediate **8** (1.0 mmol) and TEA (3.0 mmol) in anhydrous DCM (8 mL) was cooled with an ice bath, then paratoluensulfonyl chloride (1.1 mmol, dissolved in 2 mL anhydrous DCM) was added dropwise. The reaction mixture was allowed to stir at 0 °C for 2 h. After removing the cooling bath, the resulting mixture was stirred for 6 h at room temperature, then diluted with saturated aqueous NaHCO₃ and extracted with DCM (10 mL) three times. The combined organic layer was sequentially washed with water and brine, dried with anhydrous Na₂SO₄, and concentrated in vacuo. The crude was purified by column chromatography with DCM/methanol to yield compounds **IIIa-o** as white solids.

4.1.11.1. 4-Fluoro-N-(4-(((2-methylphenyl)sulfonamido)methyl)benzyl)benzamide (IIIa): White solid, yield 75%, m.p. 144-146 °C. ¹H NMR (600 MHz, DMSO-d₆) δ 9.04 (t, J = 6.0 Hz, 1H), 8.19 (d, J = 5.6 Hz, 1H), 7.94 – 7.97 (m, 2H), 7.80 (dd, J = 7.9, 1.3 Hz, 1H), 7.47 (td, J = 7.5, 1.4 Hz, 1H), 7.29 – 7.36 (m, 4H), 7.18 (dd, J = 8.1, 34.8 Hz, 4H), 4.42 (d, J = 5.9 Hz, 2H), 3.97 (d, J = 4.9 Hz, 2H), 2.55 (s, 3H). ¹³C NMR (100 MHz, DMSO-d₆) δ 165.11, 165.06, 162.63, 138.89, 138.47, 136.43, 136.39, 132.43, 132.32, 130.81, 130.78, 129.91, 129.82, 128.32, 127.47, 127.09, 126.16, 115.34, 115.13, 45.60, 42.37, 19.82. HRMS calcd for C₂₂H₂₂O₃N₂SF 413.13297 [M + H]⁺, found 413.13310.

4.1.11.2. 4-Fluoro-N-(4-(((3-methylphenyl)sulfonamido)methyl)benzyl)benzamide (IIIb): White solid, yield 79%, m.p. 171-173 °C. ¹H NMR (400 MHz, DMSO-d₆) δ 9.05 (t, J = 6.0 Hz, 1H), 8.07 (s, 1H), 7.94 – 7.97 (m, 2H), 7.59 (d, J = 5.6 Hz, 2H), 7.40 – 7.47 (m, 2H), 7.31 (t, J = 8.8 Hz, 2H), 7.20 (dd, J = 19.2, 8.0 Hz, 4H), 4.43 (d, J = 6.0 Hz, 2H), 3.94 (s, 2H), 2.36 (s, 3H). ¹³C NMR (100 MHz, DMSO-d₆) δ 165.07, 165.04, 162.60, 140.59, 138.76, 138.49, 136.13, 132.84, 130.79, 130.77, 129.88, 129.79, 128.97, 127.54, 127.10, 126.70, 123.56, 115.30, 115.08, 45.88, 42.35, 20.81. HRMS calcd for C₂₂H₂₂O₃N₂SF 413.13297 [M + H]⁺, found 413.13233.

4.1.11.3. 4-Fluoro-N-(4-(((2-fluorophenyl)sulfonamido)methyl)benzyl)benzamide (IIIc): White solid, yield 88%, m.p. 133-135 °C. ¹H NMR (600 MHz, DMSO-d₆) δ 9.04 (t, J = 6.0 Hz, 1H), 8.47 (s, 1H), 7.94 – 7.98 (m, 2H), 7.73 – 7.76 (m, 1H), 7.60 – 7.64 (m, 1H), 7.29 – 7.37 (m, 4H), 7.18 (dd, J = 8.2, 18.0 Hz, 4H), 4.41 (d, J = 6.0 Hz, 2H), 4.08 (s, 2H). ¹³C NMR (100 MHz, DMSO-d₆) δ 165.11, 165.06, 162.64, 159.33, 156.81, 138.50, 136.09, 135.07, 134.98, 130.81, 130.78, 129.91, 129.82, 129.52, 128.84, 128.70, 127.44, 127.10, 124.76, 124.73, 117.21, 117.00, 115.35, 115.13, 45.69, 42.36. HRMS calcd for C₂₁H₁₉O₃N₂SF₂ 417.10790 [M + H]⁺, found 417.10751.

4.1.11.4. 4-Fluoro-N-(4-(((3-fluorophenyl)sulfonamido)methyl)benzyl)benzamide

(III_d): White solid, yield 82%, m.p. 164-166 °C. ¹H NMR (400 MHz, DMSO-d₆) δ 9.05 (t, J = 6.0 Hz, 1H), 8.27 (t, J = 6.3 Hz, 1H), 7.93 – 7.98 (m, 2H), 7.59 – 7.65 (m, 2H), 7.54 – 7.57 (m, 1H), 7.45 – 7.50 (m, 1H), 7.28 – 7.34 (m, 2H), 7.20 (dd, J = 19.6, 8.2 Hz, 4H), 4.42 (d, J = 6.0 Hz, 2H), 3.98 (d, J = 6.2 Hz, 2H). ¹³C NMR (100 MHz, DMSO-d₆) δ 165.07, 162.94, 162.65, 160.48, 142.88, 142.81, 138.66, 135.87, 131.64, 131.56, 130.80, 130.77, 129.93, 129.84, 127.64, 127.17, 119.59, 119.37, 115.38, 115.16, 113.63, 113.39, 109.58, 45.93, 42.37. HRMS calcd for C₂₁H₁₉O₃N₂SF₂ 417.10790 [M + H]⁺, found 417.10812.

4.1.11.5. 4-Fluoro-N-(4-(((4-fluorophenyl)sulfonamido)methyl)benzyl)benzamide

(III_e): White solid, yield 80%, m.p. 170-172 °C. ¹H NMR (600 MHz, DMSO-d₆) δ 9.05 (t, J = 6.0 Hz, 1H), 8.17 (s, 1H), 7.94 – 7.97 (m, 2H), 7.82 – 7.85 (m, 2H), 7.38 – 7.42 (m, 2H), 7.28 – 7.32 (m, 2H), 7.20 (dd, J = 8.1, 31.2 Hz, 4H), 4.42 (d, J = 5.9 Hz, 2H), 3.95 (s, 2H). ¹³C NMR (100 MHz, DMSO-d₆) δ 165.27, 165.10, 165.07, 162.77, 162.63, 138.60, 137.11, 137.08, 135.94, 130.79, 130.77, 129.91, 129.82, 129.51, 129.42, 127.60, 127.15, 116.37, 116.15, 115.33, 115.11, 45.90, 42.38. HRMS calcd for C₂₁H₁₉O₃N₂SF₂ 417.10790 [M + H]⁺, found 417.10765.

4.1.11.6. 4-Fluoro-N-(4-(((2-chlorophenyl)sulfonamido)methyl)benzyl)benzamide

(III_f): White solid, yield 77%, m.p. 128-130 °C. ¹H NMR (600 MHz, DMSO-d₆) δ 9.03 (t, J = 6.0 Hz, 1H), 8.42 (t, J = 6.0 Hz, 1H), 7.94 – 7.97 (m, 2H), 7.90 (dd, J = 7.8, 1.6 Hz, 1H), 7.53 – 7.59 (m, 2H), 7.44 – 7.47 (m, 1H), 7.29 – 7.32 (m, 2H), 7.17 (dd, J = 13.5, 8.1 Hz, 4H), 4.40 (d, J = 6.0 Hz, 2H), 4.06 (d, J = 5.7 Hz, 2H). ¹³C NMR (100 MHz, DMSO-d₆) δ 165.11, 165.05, 162.64, 138.49, 138.25, 136.08, 133.75, 131.62, 130.81, 130.78, 130.58, 130.31, 129.91, 129.82, 127.51, 127.47, 127.04, 115.35, 115.14, 45.79, 42.35. HRMS calcd for C₂₁H₁₉O₃N₂SFCl 433.07835 [M + H]⁺, found 433.07837.

4.1.11.7. 4-Fluoro-N-(4-(((3-chlorophenyl)sulfonamido)methyl)benzyl)benzamide

(III_g): White solid, yield 80%, m.p. 160-162 °C. ¹H NMR (600 MHz, DMSO-d₆) δ 9.04 (t, J = 6.0 Hz, 1H), 8.29 (s, 1H), 7.94 – 7.97 (m, 2H), 7.72 – 7.74 (m, 2H), 7.66 – 7.68 (m, 1H), 7.58 (t, J = 7.9 Hz, 1H), 7.29 – 7.32 (m, 2H), 7.19 (dd, J = 7.9, 28.8 Hz, 4H), 4.42 (d, J = 6.0 Hz, 2H), 3.99 (s, 2H). ¹³C NMR (100 MHz, DMSO-d₆) δ 165.48, 163.05, 143.08, 139.08, 136.19, 134.15, 132.66, 131.63, 131.23, 131.20, 130.33, 130.24, 128.06, 127.58, 126.52, 125.57, 115.76, 115.55, 46.35, 42.79. HRMS calcd for C₂₁H₁₉O₃N₂SCl 433.07835 [M + H]⁺, found 433.07849.

4.1.11.8. 4-Fluoro-N-(4-(((4-chlorophenyl)sulfonamido)methyl)benzyl)benzamide

(III_h): White solid, yield 82%, m.p. 169-171 °C. ¹H NMR (600 MHz, DMSO-d₆) δ 9.05 (t, J = 6.0 Hz, 1H), 8.23 (s, 1H), 7.94 – 7.97 (m, 2H), 7.76 – 7.79 (m, 2H), 7.63 – 7.65 (m, 2H), 7.28 – 7.32 (m, 2H), 7.20 (dd, J = 8.1, 30.6 Hz, 4H), 4.43 (d, J = 6.0 Hz, 2H), 3.96 (s, 2H). ¹³C NMR (100 MHz, DMSO-d₆) δ 165.06, 139.57, 138.63, 137.15, 135.88, 130.79, 130.76, 129.91, 129.82, 129.27, 128.42, 127.60, 127.15, 115.32, 115.10, 45.89, 42.37. HRMS calcd for C₂₁H₁₉O₃N₂SFCl 433.07835 [M + H]⁺, found 433.07809.

4.1.11.9. 4-Fluoro-N-(4-(((4-nitrophenyl)sulfonamido)methyl)benzyl)benzamide

(III_i): White solid, yield 60%, m.p. 186-188 °C. ¹H NMR (400 MHz, DMSO-d₆) δ 9.05 (t,

J = 6.0 Hz, 1H), 8.53 (s, 1H), 8.35 – 8.39 (m, 2H), 7.99 – 8.02 (m, 2H), 7.93 – 7.96 (m, 2H), 7.28 – 7.33 (m, 2H), 7.19 (dd, J = 18.4, 8.1 Hz, 4H), 4.40 (d, J = 5.9 Hz, 2H), 4.02 (s, 2H). ¹³C NMR (100 MHz, DMSO-d₆) δ 165.06, 162.63, 149.43, 146.32, 138.74, 135.63, 130.77, 130.74, 129.90, 129.81, 128.04, 127.66, 127.15, 124.48, 115.32, 115.11, 45.93, 42.34. HRMS calcd for C₂₁H₁₉O₅N₃SF 444.10240 [M + H]⁺, found 444.10239.

4.1.11.10. 4-Fluoro-N-(4-(((3-

(trifluoromethyl)phenyl)sulfonamido)methyl)benzyl)benzamide (IIIj): White solid, yield 65%, m.p. 170-172 °C. ¹H NMR (400 MHz, DMSO-d₆) δ 9.04 (t, J = 6.0 Hz, 1H), 8.40 (t, J = 5.8 Hz, 1H), 7.93 – 8.04 (m, 5H), 7.78 (t, J = 7.8 Hz, 1H), 7.31 (t, J = 8.9 Hz, 2H), 7.16 (dd, J = 17.2, 7.6 Hz, 4H), 4.39 (d, J = 5.9 Hz, 2H), 4.02 (d, J = 5.2 Hz, 2H). ¹³C NMR (100 MHz, DMSO-d₆) δ 165.03, 162.62, 142.06, 138.64, 135.57, 130.78, 130.75, 130.71, 130.48, 129.89, 129.86, 129.80, 129.53, 128.97, 128.93, 127.62, 127.14, 124.77, 123.00, 122.96, 115.32, 115.10, 45.92, 42.32. HRMS calcd for C₂₂H₁₉O₃N₂SF₄ 467.10470 [M + H]⁺, found 467.10488.

4.1.11.11. 4-Fluoro-N-(4-(((3,4-difluorophenyl)sulfonamido)methyl)benzyl)benzamide

(IIIk): White solid, yield 70%, m.p. 165-167 °C. ¹H NMR (400 MHz, DMSO-d₆) δ 9.06 (t, J = 6.0 Hz, 1H), 8.29 (s, 1H), 7.93 – 7.97 (m, 2H), 7.77 – 7.81 (m, 1H), 7.62 – 7.66 (m, 2H), 7.30 (t, J = 8.9 Hz, 2H), 7.20 (dd, J = 22.4, 8.0 Hz, 4H), 4.42 (d, J = 5.9 Hz, 2H), 4.00 (s, 2H). ¹³C NMR (100 MHz, DMSO-d₆) δ 165.08, 162.65, 150.44, 138.71, 137.97, 135.75, 130.80, 130.77, 129.93, 129.84, 127.69, 127.18, 124.38, 124.34, 124.30, 124.26, 118.68, 118.50, 116.48, 116.29, 115.36, 115.15, 45.95, 42.37. HRMS calcd for C₂₁H₁₈O₃N₂SF₃ 435.09847 [M + H]⁺, found 435.09855.

4.1.11.12. 4-Fluoro-N-(4-((pyridine-3-sulfonamido)methyl)benzyl)benzamide

(IIIll): White solid, yield 50%, m.p. 165-167 °C. ¹H NMR (400 MHz, DMSO-d₆) δ 9.05 (t, J = 6.0 Hz, 1H), 8.91 (d, J = 2.5 Hz, 1H), 8.75 (dd, J = 4.8, 1.4 Hz, 1H), 8.40 (t, J = 6.0 Hz, 1H), 8.08 – 8.11 (m, 1H), 7.93 – 7.97 (m, 2H), 7.56 (dd, J = 8.0, 4.9 Hz, 1H), 7.28 – 7.34 (m, 2H), 7.18 (d, J = 17.6, 8.1 Hz, 4H), 4.41 (d, J = 5.9 Hz, 2H), 4.02 (d, J = 5.7 Hz, 2H). ¹³C NMR (100 MHz, DMSO-d₆) δ 165.10, 165.05, 162.62, 152.80, 146.97, 138.64, 137.17, 135.68, 134.39, 130.79, 130.76, 129.90, 129.81, 127.62, 127.16, 124.14, 115.34, 115.12, 45.87, 42.34. HRMS calcd for C₂₀H₁₉O₃N₃SF 400.11257 [M + H]⁺, found 400.11220.

4.1.11.13. 4-Fluoro-N-(4-(((2,3-dihydrobenzofuran)-5-

sulfonamido)methyl)benzyl)benzamide (IIIIm): White solid, yield 79%, m.p. 215-217 °C. ¹H NMR (400 MHz, DMSO-d₆) δ 9.06 (t, J = 6.0 Hz, 1H), 7.93 – 7.98 (m, 2H), 7.90 (t, J = 6.4 Hz, 1H), 7.60 (m, 1H), 7.55 (dd, J = 8.4, 2.1 Hz, 1H), 7.28 – 7.34 (m, 2H), 7.20 (dd, J = 19.2, 8.2 Hz, 4H), 6.90 (d, J = 8.4 Hz, 1H), 4.62 (t, J = 8.8 Hz, 2H), 4.43 (d, J = 5.9 Hz, 2H), 3.89 (d, J = 6.3 Hz, 2H), 3.22 (t, J = 8.8 Hz, 2H). ¹³C NMR (100 MHz, DMSO-d₆) δ 165.09, 165.06, 162.77, 162.62, 138.46, 136.22, 132.22, 129.90, 129.81, 128.63, 127.77, 127.58, 127.07, 123.95, 115.33, 115.11, 108.94, 72.09, 45.90, 42.36, 28.46. HRMS calcd for C₂₃H₂₂O₄N₂SF 441.12788 [M + H]⁺, found 441.12788.

4.1.11.14. 4-Fluoro-N-(4-((naphthalene-1-sulfonamido)methyl)benzyl)benzamide

(IIIIn): White solid, yield 72%, m.p. 143-145 °C. ¹H NMR (400 MHz, DMSO-d₆) δ 9.01 (t,

J = 6.0 Hz, 1H), 8.67 (d, J = 8.0 Hz, 1H), 8.49 (s, 1H), 8.18 (d, J = 8.3 Hz, 1H), 8.10 (dd, J = 7.4, 1.3 Hz, 1H), 8.06 (d, J = 8.0 Hz, 1H), 7.93 – 7.97 (m, 2H), 7.58 – 7.73 (m, 3H), 7.28 – 7.33 (m, 2H), 7.15 (dd, J = 17.4, 8.2 Hz, 4H), 4.38 (d, J = 6.0 Hz, 2H), 3.99 (s, 2H). ¹³C NMR (100 MHz, DMSO-d₆) δ 165.07, 165.01, 162.59, 138.39, 136.16, 135.75, 133.81, 133.58, 130.79, 130.76, 129.87, 129.78, 128.86, 128.34, 127.73, 127.49, 127.37, 126.96, 126.75, 124.72, 124.44, 115.29, 115.07, 45.68, 42.31. HRMS calcd for C₂₅H₂₂O₃N₂SF 449.13297 [M + H]⁺, found 449.13243.

4.1.11.15. 4-Fluoro-N-(4-(((4'-fluoro-[1,1'-biphenyl])-4-

sulfonamido)methyl)benzyl)benzamide (IIIo): White solid, yield 77%, m.p. 189-191 °C. ¹H NMR (400 MHz, DMSO-d₆) δ 9.05 (t, J = 6.0 Hz, 1H), 8.18 (t, J = 6.0 Hz, 1H), 7.93 – 7.96 (m, 2H), 7.86 (s, 4H), 7.78 – 7.81 (m, 2H), 7.28 – 7.37 (m, 4H), 7.22 (dd, J = 13.2, 8.4 Hz, 4H), 4.42 (d, J = 5.9 Hz, 2H), 3.97 (d, J = 5.2 Hz, 2H). ¹³C NMR (100 MHz, DMSO-d₆) δ 165.06, 163.64, 162.61, 161.19, 142.78, 139.39, 138.56, 136.10, 135.05, 135.02, 130.78, 130.76, 129.89, 129.80, 129.24, 129.16, 127.58, 127.33, 127.16, 127.14, 116.07, 115.85, 115.32, 115.10, 45.91, 42.37. HRMS calcd for C₂₇H₂₃O₃N₂SF₂ 493.13920 [M + H]⁺, found 493.13953.

4.2. Primary binding affinity screening

For binding affinity assay, 2 × 10⁴ MDA-MB-231 cells in 300 μL of cell culture medium were seeded in an 8-well slide chamber two days before the experiments were conducted. Various concentrations of different compounds (1, 10, 100, or 1000 nM) were added to the separate wells and incubated for 10 minutes at room temperature, and then the cells were fixed in 4% ice-cold paraformaldehyde. The cells were rehydrated in phosphate-buffered saline (PBS). The slides were subsequently incubated for 30 minutes at room temperature with 0.05 μg/mL biotinylated TN14003, washed three times with PBS, and incubated in streptavidin-rhodamine (1:150 dilution; Jackson ImmunoResearch Laboratories, West Grove, PA) for 30 minutes at room temperature. Finally, the slides were washed with PBS and mounted in an anti-fade mounting solution (Molecular Probes, Eugene, OR), and the samples were analyzed on a Nikon Eclipse E800 microscope [18-23, 26].

4.3. Matrigel invasion assay

Matrigel invasion assay was performed by using a Matrigel invasion chamber from Corning Biocoat (Bedford, MA). CXCL12α (200 ng/mL; R & D Systems, Minneapolis, MN) was added to the bottom chamber to induce the invasion of MDA-MB-231 cells through the Matrigel. The selected compounds (100 nM) or AMD3100 were added to the cells before the cells were seeded in the top chamber. The Matrigel invasion chamber was incubated for 22 hours in a humidified cell culture incubator. First, non-invading cells were removed from the top of the Matrigel with a cotton-tipped swab. Invading cells on the filter at the bottom of the Matrigel were fixed in methanol and stained with hematoxylin and eosin (H & E). The percent of invasion was determined by counting the H&E stained cells [18-23].

4.4. Carrageenan-induced paw inflammation suppression test

Acute inflammation was induced by subcutaneous injection of 50 μL of λ-carrageenan (1% w/v in saline) into one of the hind paws of the female C57BL/6J mice (Jackson

Laboratories); the other hind paw was injected with 50 μ L of saline, which was used as a non-inflammation control. The selected compounds were dissolved in 10% DMSO and 90% of 45% (2-hydroxypropyl)- β -cyclodextrin (CD) in PBS. In the treatment group, compounds **IIb**, **IIc**, **IIIg**, **IIIj**, **IIIm** and RB-108 were administered intraperitoneally (i.p.) at 10 mg/kg daily, 30 minutes following carrageenan challenge. Control animals received the corresponding i.p. injections of the vehicle. The animals were sacrificed 74 hours after carrageenan challenge and 2 hours after the last injection of the selected compounds. The final paws were photographed and measured for thickness from the “palm” to the back of the paw with a caliper. These were compared to the volume of the carrageenan-untreated contralateral paw to obtain the edema volume; the volume of the contralateral paw was subtracted from the volume of the carrageenan-injected paw to obtain the edema volume. The inflammation-suppression percentage was calculated by comparing the drug-treated group to the control group. Five mice per group were used to determine the effect of the anti-CXCR4 compounds as previously described [20, 26].

4.5. Preliminary pharmacokinetic study of compound **III**m

Compound **III**m (10% DMSO and 90% PBS) was administered to 2 male SD rats at doses of 10 mg/kg via intragastric administration. After administration, blood samples were collected at the time points of 5 min, 15 min, 30 min, 1 h, 2 h, 4 h, and 6 h for analyses, the collected blood samples were centrifuged at 4000 rpm for 5 min at 4 °C and then analyzed after protein precipitation. LC/MS/MS analysis of compounds was performed under optimized conditions to obtain the best sensitivity and selectivity of the analyte in the selected reaction monitoring mode (SRM) containing an internal standard. Plasma concentration-time data were measured by a noncompartmental approach using the software WinNonlin Enterprise, version 6.4 [25].

4.6. Preliminary cytotoxicity study of compound **III**m

The antiproliferative activity of the compounds was determined using the MTT assay. Cells were seeded in 96-well micro culture plates at 3000 cells/well in 100 μ L of medium and incubated for 24 h at 37 °C in a CO₂ incubator. Following the incubation for 24 h, these cells were treated with Compound **III**m for 24 h at 37 °C. Finally, 20 μ L of CellTiter 96AQ reagent (Promega, Madison, WI) was added into each well and incubated for an additional 2 h, and the absorbance at 490 nm was measured.

Supplementary Material

Refer to Web version on PubMed Central for supplementary material.

Acknowledgments

This study was financially supported by the National Natural Science Foundation of China, NSFC (Grant No. 81803340), Zhejiang Provincial Department of Education (Grant No. Y201840109) and NIH NCI (R01 CA165306).

References

- [1]. Schmidt D, Bemat V, Brox R, Tschammer N, Kolb P, Identifying modulators of CXC receptors 3 and 4 with tailored selectivity using multi-target docking, *ACS Chem. Biol* 10 (2015) 715–724. [PubMed: 25398025]
- [2]. Kircher M, Herhaus P, Schottelius M, Buck AK, Werner RA, Wester HJ, Keller U, Lapa C, CXCR4-directed theranostics in oncology and inflammation, *Ann. Nucl. Med* 32 (2018) 503–511. [PubMed: 30105558]
- [3]. Gross A, Brox R, Damm D, Tschammer N, Schmidt B, Eichler J, Ligand selectivity of a synthetic CXCR4 mimetic peptide, *Bioorg. Med. Chem* 23 (2015) 4050–4055. [PubMed: 25801155]
- [4]. Hummel S, Van Aken H, Zarbock A, Inhibitors of CXC chemokine receptor type 4: putative therapeutic approaches in inflammatory diseases, *Curr. Opin. Hematol* 21 (2014) 29–36. [PubMed: 24275689]
- [5]. Choi WT, Duggineni S, Xu Y, Huang Z, An J, Drug discovery research targeting the CXC chemokine receptor 4 (CXCR4), *J. Med. Chem* 55 (2012) 977–994. [PubMed: 22085380]
- [6]. Chatterjee S, Behnam Azad B, Nimmagadda S, The intricate role of CXCR4 in cancer, *Adv. Cancer Res* 124 (2014) 31–82. [PubMed: 25287686]
- [7]. Kolaric A, Svajger U, Tomasic T, Brox R, Frank T, Minovski N, Tschammer N, Anderluh M, Insight into structural requirements for selective and/or dual CXCR3 and CXCR4 allosteric modulators, *Eur. J. Med. Chem* 154 (2018) 68–90. [PubMed: 29777988]
- [8]. Shi H, Lu R, Wang S, Chen H, Wang F, Liu K, Effects of SDF-1/CXCR4 on Acute Lung Injury Induced by Cardiopulmonary Bypass, *Inflammation* 40 (2017) 937–945. [PubMed: 28285461]
- [9]. Furze RC, Rankin SM, Neutrophil mobilization and clearance in the bone marrow, *Immunology* 125 (2008) 281–288. [PubMed: 19128361]
- [10]. Nagafuchi Y, Shoda H, Sumitomo S, Nakachi S, Kato R, Tsuchida Y, Tsuchiya H, Sakurai K, Hanata N, Tateishi S, Kanda H, Ishigaki K, Okada Y, Suzuki A, Kochi Y, Fujio K, Yamamoto K, Immunophenotyping of rheumatoid arthritis reveals a linkage between HLA-DRB1 genotype, CXCR4 expression on memory CD4(+) T cells, and disease activity, *Sci. Rep* 6 (2016) 29338. [PubMed: 27385284]
- [11]. Zraggen S, Huggenberger R, Kerl K, Detmar M, An important role of the SDF-1/CXCR4 axis in chronic skin inflammation, *PloS one* 9 (2014) e93665. [PubMed: 24695674]
- [12]. Donzella GA, Schols D, Lin SW, Este JA, Nagashima KA, Maddon PJ, Allaway GP, Sakmar TP, Henson G, De Clercq E, Moore JP, AMD3100, a small molecule inhibitor of HIV-1 entry via the CXCR4 co-receptor, *Nat. Med* 4 (1998) 72–77. [PubMed: 9427609]
- [13]. Lefrancois M, Lefebvre MR, Saint-Onge G, Boulais PE, Lamothe S, Leduc R, Lavigne P, Heveker N, Escher E, Agonists for the Chemokine Receptor CXCR4, *ACS Med. Chem. Lett* 2 (2011) 597–602. [PubMed: 21841963]
- [14]. Scozzafava A, Mastrolorenzo A, Supuran CT, Non-peptidic chemokine receptors antagonists as emerging anti-HIV agents, *J. Enzyme Inhib. Med. Chem* 17 (2002) 69–76. [PubMed: 12420752]
- [15]. Hendrix CW, Flexner C, MacFarland RT, Giandomenico C, Fuchs EJ, Redpath E, Bridger G, Henson GW, Pharmacokinetics and safety of AMD-3100, a novel antagonist of the CXCR-4 chemokine receptor, in human volunteers, *Antimicrob. Agents Chemother* 44 (2000) 1667–1673. [PubMed: 10817726]
- [16]. De Clercq E, The bicyclam AMD3100 story, *Nature reviews. Drug Disc.* 2 (2003) 581–587.
- [17]. Liang Z, Zhan W, Zhu A, Yoon Y, Lin S, Sasaki M, Klapproth JM, Yang H, Grossniklaus HE, Xu J, Rojas M, Voll RJ, Goodman MM, Arrendale RF, Liu J, Yun CC, Snyder JP, Liotta DC, Shim H, Development of a unique small molecule modulator of CXCR4, *PloS one* 7 (2012) e34038. [PubMed: 22485156]
- [18]. Bai R, Shi Q, Liang Z, Yoon Y, Han Y, Feng A, Liu S, Oum Y, Yun CC, Shim H, Development of CXCR4 modulators by virtual HTS of a novel amide-sulfamide compound library, *Eur. J. Med. Chem* 126 (2017) 464–475. [PubMed: 27914361]
- [19]. Bai R, Sun J, Liang Z, Yoon Y, Salgado E, Feng A, Oum Y, Xie Y, Shim H, Anti-inflammatory hybrids of secondary amines and amide-sulfamide derivatives, *Eur. J. Med. Chem* 150 (2018) 195–205. [PubMed: 29529500]

- [20]. Bai R, Liang Z, Yoon Y, Liu S, Gaines T, Oum Y, Shi Q, Mooring SR, Shim H, Symmetrical bis-tertiary amines as novel CXCR4 inhibitors, *Eur. J. Med. Chem* 118 (2016) 340–350. [PubMed: 27179215]
- [21]. Bai R, Liang Z, Yoon Y, Salgado E, Feng A, Gurbani S, Shim H, Novel anti-inflammatory agents targeting CXCR4: Design, synthesis, biological evaluation and preliminary pharmacokinetic study, *Eur. J. Med. Chem* 136 (2017) 360–371. [PubMed: 28521261]
- [22]. Gaines T, Camp D, Bai R, Liang Z, Yoon Y, Shim H, Mooring SR, Synthesis and evaluation of 2,5 and 2,6 pyridine-based CXCR4 inhibitors, *Bioorg. Med. Chem* 24 (2016) 5052–5060. [PubMed: 27576294]
- [23]. Mooring SR, Liu J, Liang Z, Ahn J, Hong S, Yoon Y, Snyder JP, Shim H, Benzenesulfonamides: a unique class of chemokine receptor type 4 inhibitors, *ChemMedChem* 8 (2013) 622–632. [PubMed: 23468189]
- [24]. Shu HK, Yoon Y, Hong S, Xu K, Gao H, Hao C, Torres-Gonzalez E, Nayra C, Rojas M, Shim H, Inhibition of the CXCL12/CXCR4-axis as preventive therapy for radiation-induced pulmonary fibrosis, *PLoS one* 8 (2013) e79768. [PubMed: 24244561]
- [25]. Xin M, Zhang L, Jin Q, Tang F, Wen J, Gu L, Cheng L, Zhao Y, Discovery of novel 4-(2-pyrimidinylamino)benzamide derivatives as highly potent and orally available hedgehog signaling pathway inhibitors, *Eur. J. Med. Chem* 110 (2016) 115–125. [PubMed: 26820554]
- [26]. Liang Z, Wu T, Lou H, Yu X, Taichman RS, Lau SK, Nie S, Umbreit J, Shim H, Inhibition of breast cancer metastasis by selective synthetic polypeptide against CXCR4, *Cancer Res.* 64 (2004) 4302–4308. [PubMed: 15205345]
- [27]. Zhu A, Zhan W, Liang Z, Yoon Y, Yang H, Grossniklaus HE, Xu J, Rojas M, Lockwood M, Snyder JP, Liotta DC, Shim H, Dipyrimidine amines: a novel class of chemokine receptor type 4 antagonists with high specificity, *J. Med. Chem* 53 (2010) 8556–8568. [PubMed: 21105715]

Highlights:

A series of CXCR4 inhibitors were synthesized based on the lead compound RB-108;

Compound **III**m significantly inhibited the invasion of CXCR4⁺ cells by 83%;

IIIm significantly attenuated mouse paw edema and tissue damage;

IIIm exhibited satisfying PK profiles with a T_{1/2} of 4.77 h.

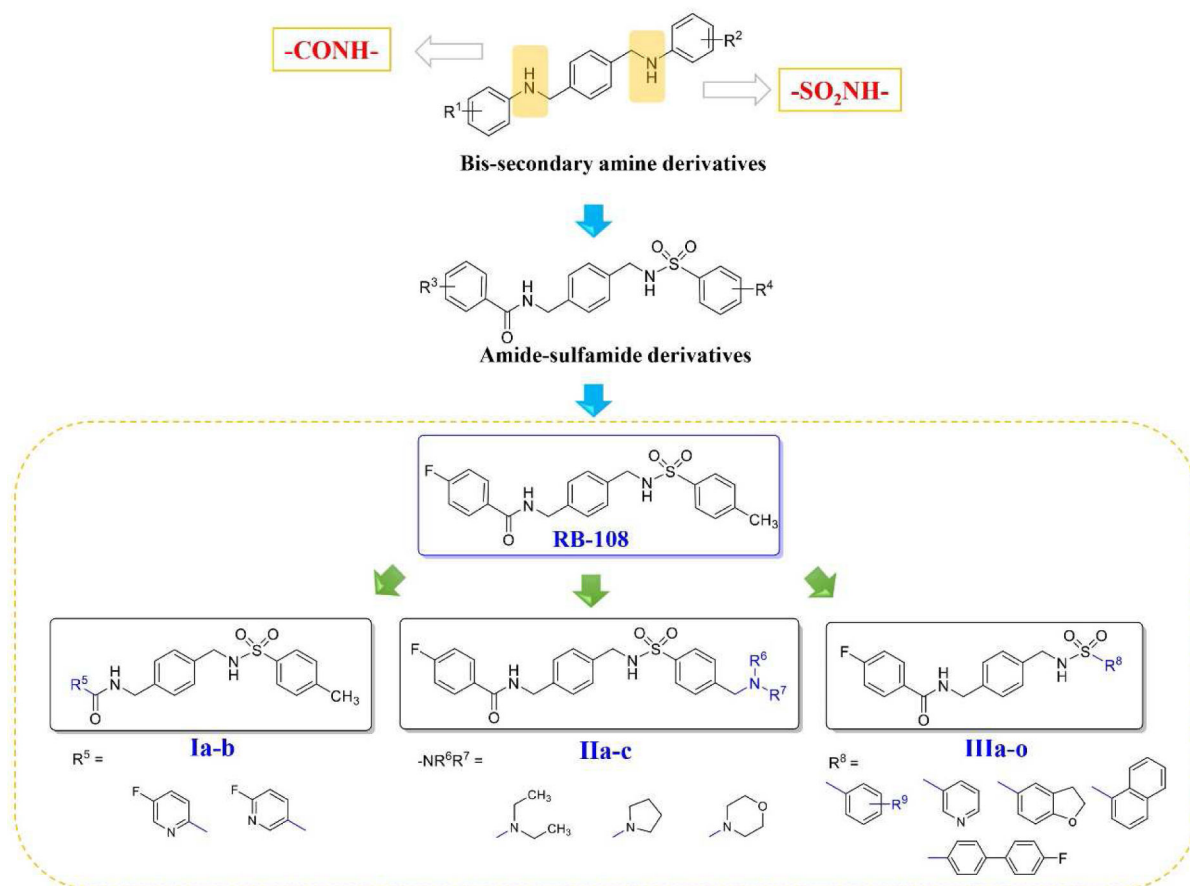


Fig. 1.
Strategy for the structural modification of the lead compound RB-108.

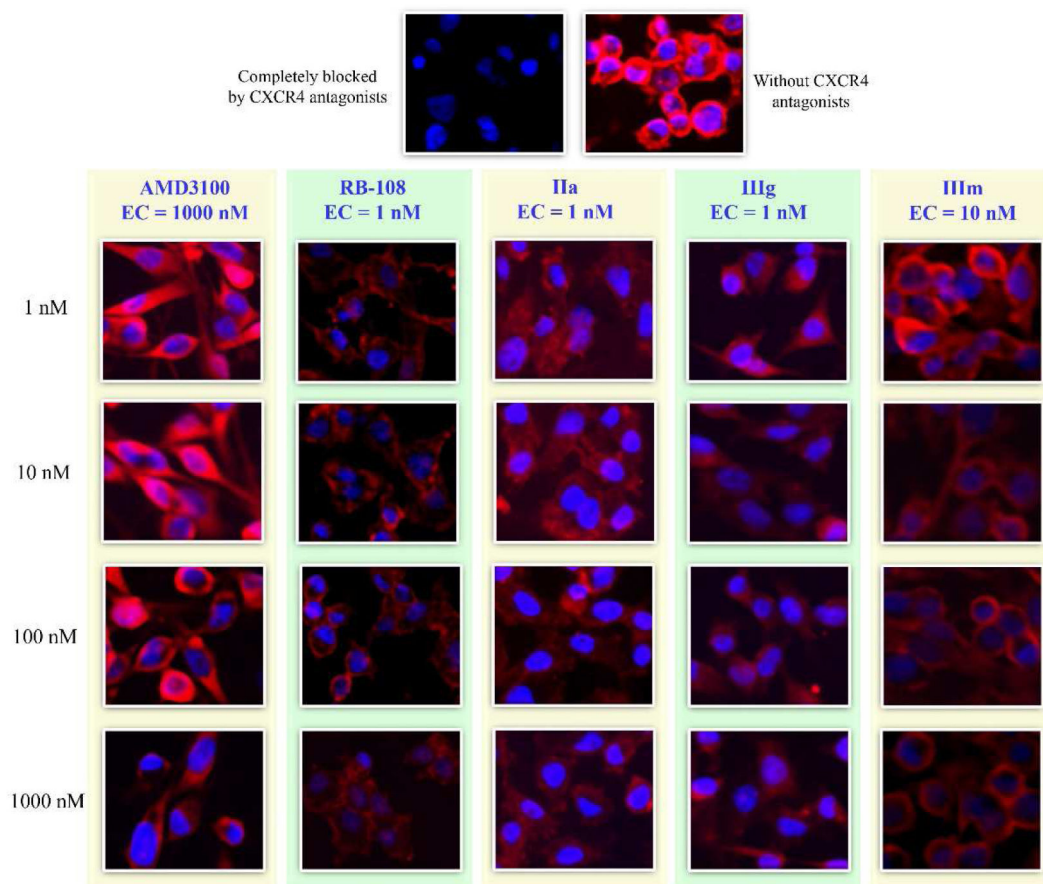


Fig. 2.

Representative immunofluorescence images of competitive-binding affinity assay of three selected compounds compared to AMD3100. When the test compounds were preincubated with the cells and blocked the binding of biotinylated TN14003, the red fluorescent color was reduced. The ECs of reference drug AMD3100 and the lead compound RB-108 were 1000 and 1 nM, respectively. Derivatives **IIa**, **IIIj** and **IIIm** exhibited ECs of only 1, 1 and 10 nM, respectively.

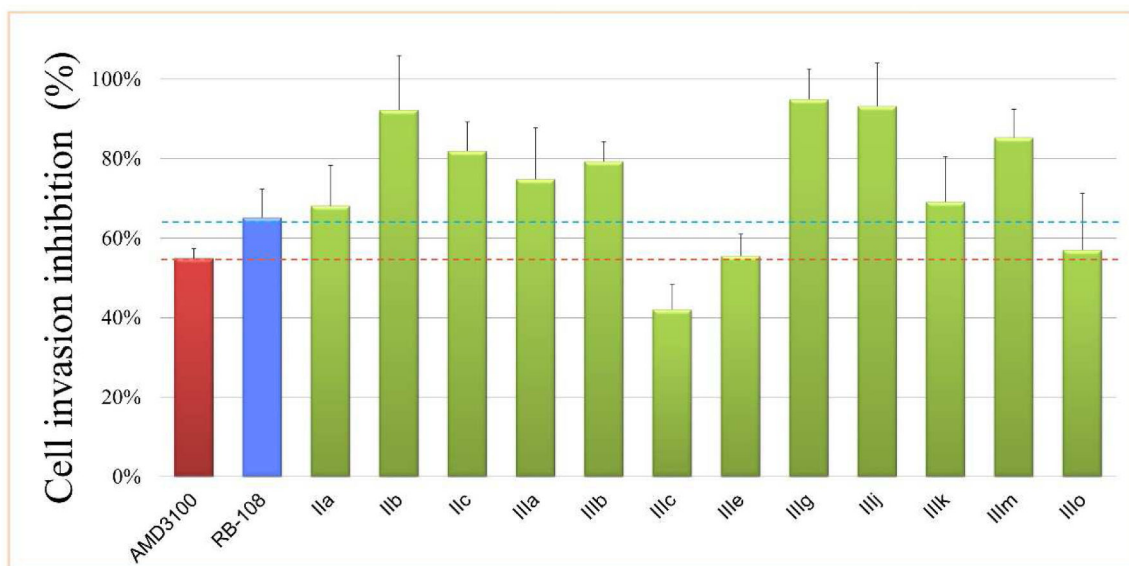


Fig. 3. Matrigel invasion assay of CXCR4⁺ cells induced by CXCR4/CXCL12-mediated interaction. CXCL12 α was added to the bottom chamber, and the compounds were added to the top chamber. After incubating for 22 h, the invading cells were fixed in methanol and stained with hematoxylin and eosin. The percent of invasion was determined by counting the stained cells.

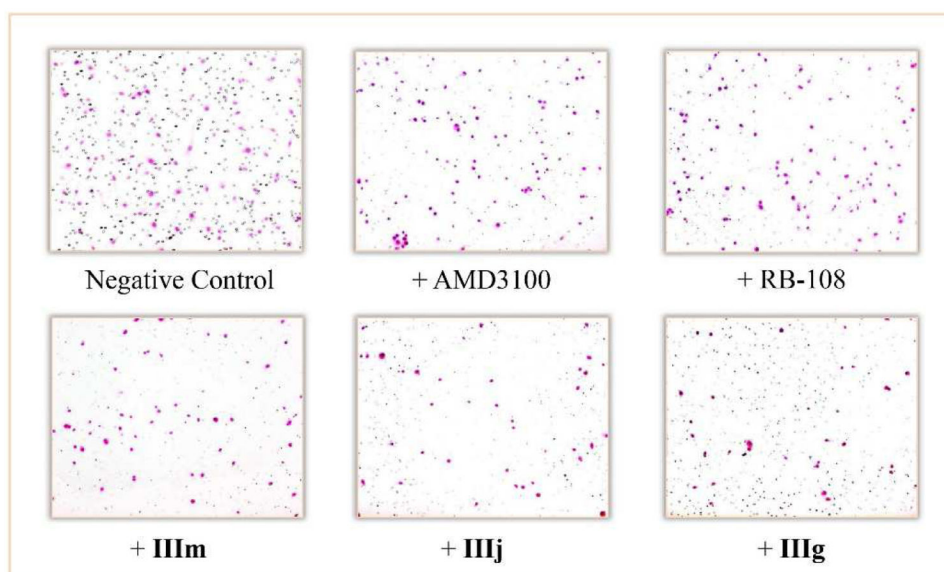


Fig. 4. Micrographs of Matrigel invasion assay induced by CXCR4/CXCL12-mediated interaction using MDA-MB-231 cells in the presence of CXCR4 inhibitors. The number of invading cells to the bottom chamber decreased when cells were incubated with our compounds in the top chamber.

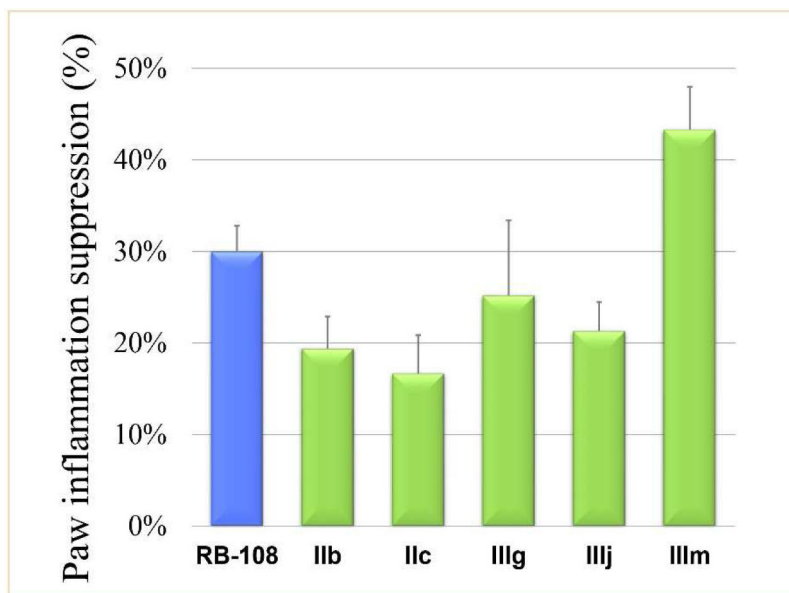


Fig. 5.
In vivo anti-inflammatory test utilizing a carrageenan-induced paw edema model.



Fig. 6. *In vivo* anti-inflammatory effect of compound **IIIIm** on carrageenan-induced mouse paw inflammation. (A) Control mouse with left paw induced inflammation by carrageenan. (B) The **IIIIm** treated mouse with left paw with left paw induced inflammation by carrageenan.

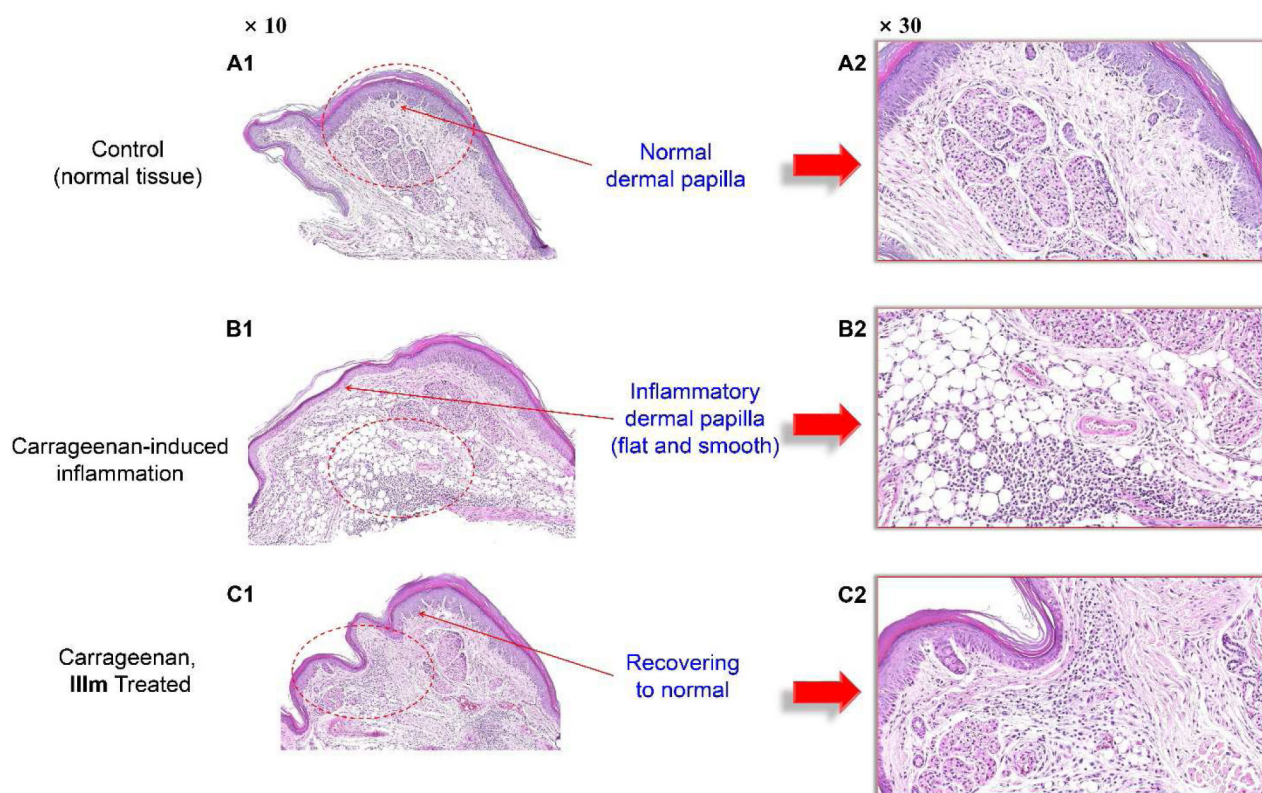


Fig. 7. Histological analysis of the *in vivo* anti-inflammatory activity of compound IIIIm. Compound IIIIm significantly attenuated the mouse paw edema and damage. The paw tissue sections were stained with H&E. The whole tissue slices were scanned/digitized by NanoZoomer 2.0 HT. Software NDP.view 2 was used to zoom in.

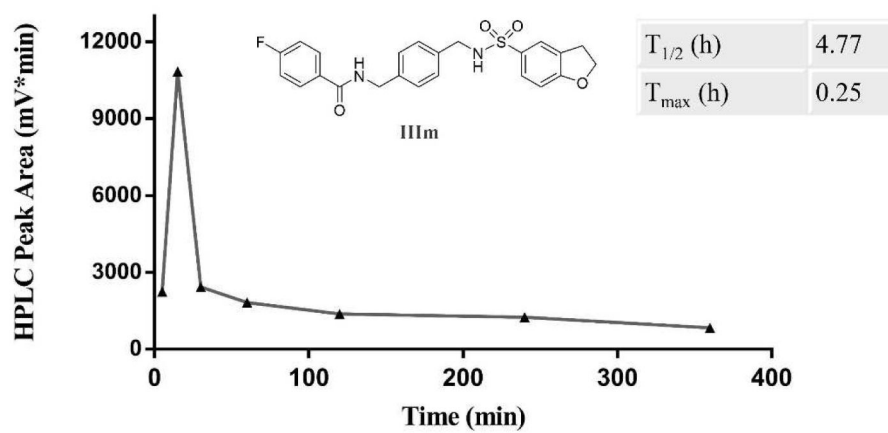


Fig. 8. Pharmacokinetic study of compound **III**m in SD rats. **III**m exhibited satisfying pharmacokinetic properties with a $T_{1/2}$ of 4.77 h

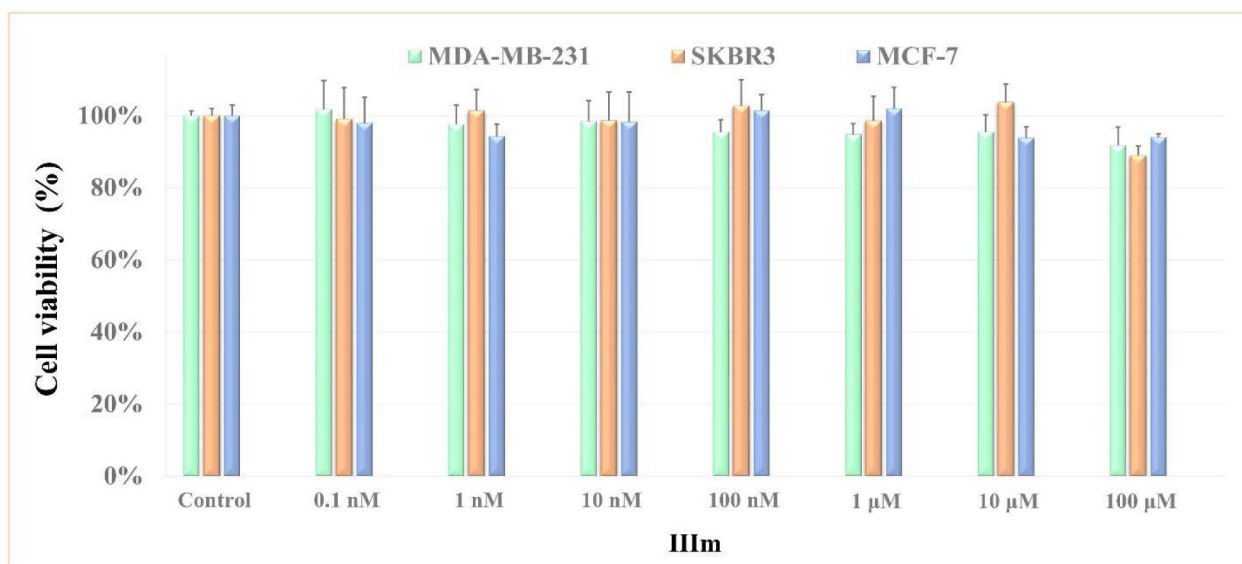
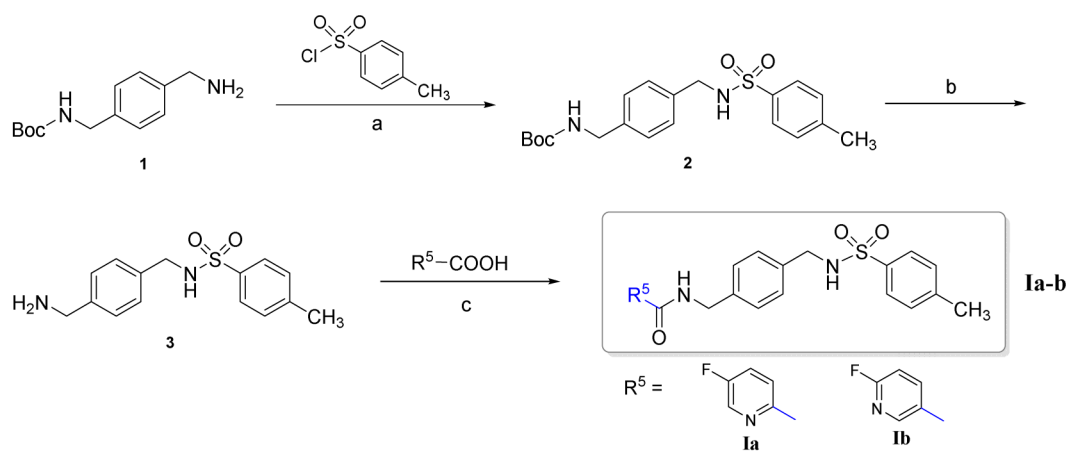
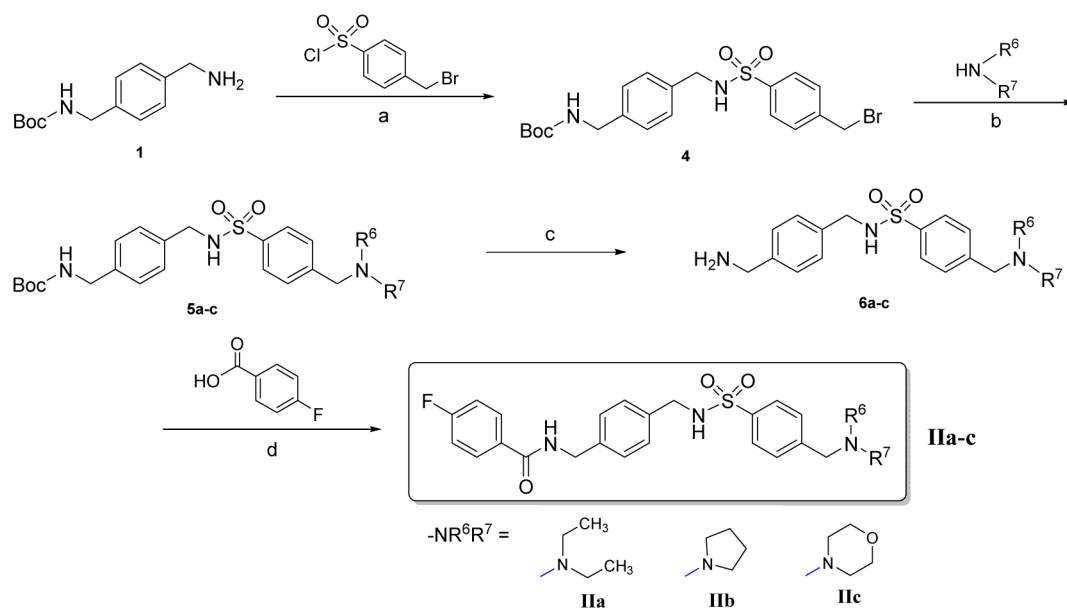


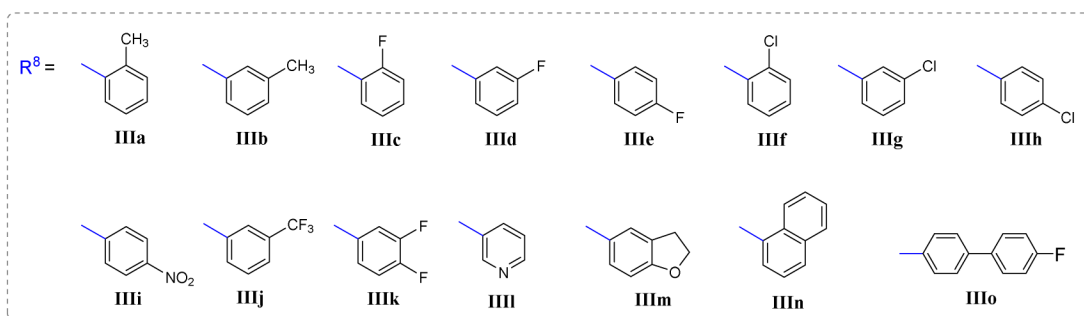
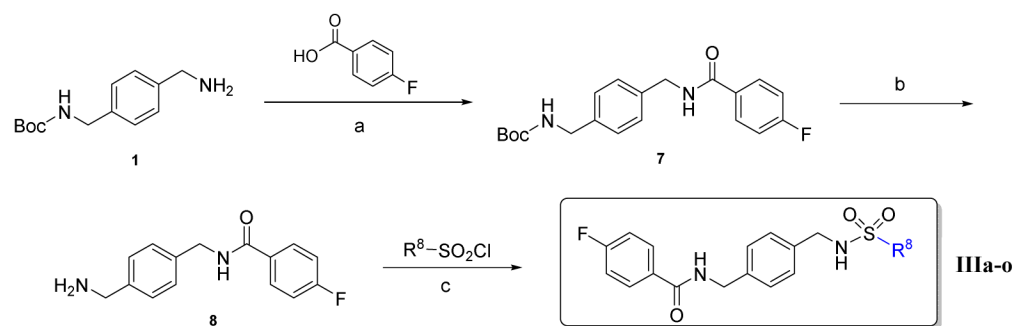
Fig. 9. Cytotoxicity evaluation of compound **III**m in MDA-MB-231, SKBR3 and MCF-7 cell lines. The antiproliferative activity of the compounds was determined using MTT assay. The results showed no statistically significant differences, which suggests that **III**m does not have antiproliferative activity.

**Scheme 1.**

Reagents and conditions: (a) DCM, TEA, ice bath to r.t., 7 h, 82%; (b) i. DCM, TFA, r.t., 8 h; ii. NaHCO_3 , 92%; (c) DCM, TEA, HOBT, EDCI, r.t., 16 h, 60-75%.

**Scheme 2.**

Reagents and conditions: (a) DCM, TEA, ice bath to r.t., 8 h, 50%; (b) CH₃CN, K₂CO₃, reflux, 4 h, 80–91%; (c) i. DCM, TFA, r.t., 8 h; ii. NaHCO₃, 87–90%; (d) DCM, TEA, HOBT, EDCI, r.t., 16 h, 77–84%.

**Scheme 3.**

Reagents and conditions: (a) DCM, TEA, HOBT, EDCI, r.t., 18 h, 87%; (b) i. DCM, TFA, r.t., 8 h ii; $NaHCO_3$, 90–95%; (c) DCM, TEA, ice bath to r.t., 8 h, 50–88%.

Table 1.

Preliminary effective concentration (EC) of anti-CXCR4 compounds.

Compound	EC (nM)	Compound	EC (nM)
Ia	1000	III f	1000
Ib	>1000	III g	1
IIa	1	III h	100
IIb	1	III i	1000
IIc	10	III j	100
IIIa	100	III k	10
IIIb	1	III l	1000
IIIc	10	III m	10
III d	1000	III n	1000
III e	1	III o	100
AMD3100	1000	RB-108	1